PCP
PLANT & CELL PHYSIOLOGY

OsPAP26 Encodes a Major Purple Acid Phosphatase and Regulates Phosphate Remobilization in Rice

Wenwen Gao[1,2], Linghong Lu[1,2], Wenmin Qiu[1,2,3], Chuang Wang[1,4] and Huixia Shou[1,*]

[1]State Key Laboratory of Plant Physiology and Biochemistry, College of Life Sciences, Zhejiang University, Hangzhou 310058, PR China
[2]These authors contributed equally to this work.
[3]Present address: Key Laboratory of Tree Breeding of Zhejiang Province, The Research Institute of Subtropical Forestry, Chinese Academy of Forestry, Hangzhou, Zhejiang 311400, PR China.
[4]Present address: College of Resources and Environment, Huazhong Agricultural University, Wuhan 430070, China.
*Corresponding author: E-mail, huixia@zju.edu.cn; Fax, +86-571-88206146.
(Received August 4, 2016; Accepted March 14, 2017)

During phosphate (Pi) starvation or leaf senescence, the accumulation of intracellular and extracellular purple acid phosphatases (PAPs) increases in plants in order to scavenge organic phosphorus (P). In this study, we demonstrated that a PAP-encoding gene in rice, *OsPAP26*, is constitutively expressed in all tissues. While the abundance of *OsPAP26* transcript is not affected by Pi supply, it is up-regulated during leaf senescence. Furthermore, Pi deprivation and leaf senescence greatly increased the abundance of OsPAP26 protein. Overexpression or RNA interference (RNAi) of *OsPAP26* in transgenic rice significantly increased or reduced APase activities, respectively, in leaves, roots and growth medium. Compared with wild-type (WT) plants, Pi concentrations of *OsPAP26*-overexpressing plants increased in the non-senescing leaves and decreased in the senescing leaves. The increased remobilization of Pi from the senescing leaves to non-senescing leaves in the *OsPAP26*-overexpressing plants resulted in better growth performance when plants were grown in Pi-depleted condition. In contrast, *OsPAP26*-RNAi plants retained more Pi in the senescing leaves, and were more sensitive to Pi starvation stress. OsPAP26 was found to localize to the apoplast of rice cells. Western blot analysis of protein extracts from callus growth medium confirmed that OsPAP26 is a secreted PAP. *OsPAP26*-overexpressing plants were capable of converting more ATP into inorganic Pi in the growth medium, which further supported the potential role of OsPAP26 in utilizing organic P in the rhizosphere. In summary, we concluded that OsPAP26 performs dual functions in plants: Pi remobilization from senescing to non-senescing leaves; and organic P utilization.

Keywords: Acid phosphatase • Organic phosphorus • OsPAP26 • Phosphate remobilization • Rice.

Abbreviations: APase, acid phosphatase; CaMV, *Cauliflower mosaic virus*; GFP, green fluorescent protein; GUS, β-glucuronidase; IAP, intracellular acid phosphatase; Oe, overexpression; P, phosphorus; PAP, purple acid phosphtase; P1BS, phosphate starvation response 1-binding sequence; PHR, phosphate starvation response transcription factor; Pi, phosphate; PSI, Pi starvation-induced; pNPP, *p*-nitrophenyl phosphate; qRT–PCR, quantitative reverse transcription–PCR; RAP, root-associated acid phosphatase; Ri, RNA interference (RNAi); SAP, secreted acid phosphatase; WT, wild type.

Introduction

Purple acid phosphatases (PAPs), a family of binuclear metal-containing acid hydrolases, have been identified in the eukaryotic kingdom which includes higher plants (Schenk et al. 2000, Olczak et al. 2003). Plant PAPs display non-specific acid phosphatase (APase) activities, which catalyze the hydrolysis of phosphate (Pi) from a broad range of organophosphates at acidic pH. Intracellular and secreted APase (IAP and SAP) activities as induced by Pi deprivation have long been recognized and studied in many plant PAPs (Miller et al. 2001, Bozzo et al. 2002, Bozzo et al. 2004a, Zhu et al. 2005, Liang et al. 2010, Zhang et al. 2011, Li et al. 2012, Tang et al. 2013, Gonzalez-Munoz et al. 2015). Pi starvation-induced (PSI) IAP and SAP are likely to be involved in the remobilization and recycling of Pi from intracellular phosphorus (P) monoesters and anhydrides of senescing tissues, or in the scavenging of Pi from organophosphate compounds in the external environment, respectively (Wang et al. 2014). Therefore, these PSI APases have important practical implications in the improvement of efficiency of P utilization in crops.

In rice, at least 24 *PAP* genes correspond to expressed sequence tag (EST) sequences in the dbEST database (Zhang et al. 2011). Among these, 10 *PAP* genes were up-regulated at the mRNA level by both phosphate deprivation and overexpression of the central transcription factor OsPHR2 (Zhang et al. 2011). Because the promoters of these PAP genes generally contain the phosphate starvation response 1-binding sequence (P1BS) elements (Zhang et al. 2011), it is likely that they are direct targets of OsPHR2. Furthermore, *OsPAP10a* and *OsPAP10c* have been fully characterized in rice (Tian et al. 2012, Lu et al. 2016). Pi deprivation led to an increase in transcript abundance of *OsPAP10a* in both leaves and roots, while the abundance of *OsPAP10c* was only up-regulated in roots. Although overexpression of *OsPAP10a* significantly increases APase activity in transgenic rice (Tian et al. 2012), OsPAP10c was demonstrated to play an additional role in the increase of APase activity and a

Plant Cell Physiol. 58(5): 885–892 (2017) doi:10.1093/pcp/pcx041, Advance Access publication on 22 March 2017, available online at www.pcp.oxfordjournals.org

plant's ability to utilize organic P in the growth medium (Lu et al. 2016). Using the protein extracts from the culture medium where the transgenic rice calli were grown, it has been confirmed that the majority of the OsPAP10c protein is secreted extracellularly (Lu et al. 2016). In addition to OsPAP10a and OsPAP10c, OsPAP15 (OsPAPhy) was found to be another fully functional phytase when expressed in *Pichia pastoris* (Dionisio et al. 2011).

More Arabidopsis PAPs have been characterized compared with rice PAPs. At least 11 out of the 29 annotated AtPAPs were found to be PSI (del Pozo et al. 1999, Haran et al. 2000, Li et al. 2002, Zhu et al. 2005, Wang et al. 2011). The Arabidopsis PSI secreted APases were further classified into: (i) SAPs that are secreted into the liquid culture medium of suspension cells or seedlings; and (ii) root-associated APases (RAPs) that are retained with the root surface after secretion. Although many RAPs are reported in various plant species (Mclachlan et al. 1980, Boutin et al. 1981, Silberbush et al. 1981), AtPAP10 is the only RAP identified in Arabidopsis (Wang et al. 2011). The expression of *AtPAP10* is induced by local and systemic Pi starvation signals in both leaves and roots (Wang et al. 2011, Zhang et al. 2014). Overexpression of *AtPAP10* enhanced plant adaptive responses to Pi limitation (Wang et al. 2011, Wang et al. 2014). AtPAP12 and AtPAP26 were reported to be the two predominant isoforms of secreted APases in the liquid culture medium of Arabidopsis suspension cells or seedlings (Veljanovski et al. 2006, Tran et al. 2010). Recently, another PAP isozyme, AtPAP25, was purified along with AtPAP12 and AtPAP26 in cell walls of Pi-starved Arabidopsis suspension cells, confirming that AtPAP25 is also a secreted PAP (Del Vecchio et al. 2014). Unlike AtPAP10, AtPAP12 and AtPAP26 that are nonspecific scavengers of organic P, AtPAP25 appears to be a phosphoprotein phosphatase that regulates Pi deprivation responses (Del Vecchio et al. 2014). In addition, AtPAP15 exhibits high phytase activity and is involved in phytate metabolism (Zhang et al. 2008, Kuang et al. 2009). Overexpression of *AtPAP15* in soybean increased the yields of transgenic soybean grown in low P soils (Wang et al. 2009).

Rice is the staple food for a large portion of the world's population. Among the 26 different *PAP* genes in rice, only *OsPAP10a* and *OsPAP10c* have been functionally characterized (Dionisio et al. 2011, Tian et al. 2012, Lu et al. 2016). In this study, we characterized the expression and functions of OsPAP26, the rice ortholog of AtPAP26. Our results indicated that OsPAP26 is a major secreted APase. It performs dual functions in rice: (i) Pi remobilization from senescing leaves to nonsenescing leaves; and (ii) utilization of organic P.

Results

Expression pattern of *OsPAP26*

Previously, we have shown that *OsPAP26* is an ortholog of *AtPAP26* in the rice genome, and that its mRNA abundance is not affected by Pi supply or the overexpression of PHR2 (Zhang et al. 2011). To confirm this result, quantitative reverse transcription–PCR (qRT–PCR) was performed. The results showed that *OsPAP26* is constitutively expressed in most tissues except the senescing leaves (**Fig. 1A**). The *OsPAP26* mRNA level in senescing leaves was about 3.6 times higher than those in the new and mature leaves, implying its potential roles in senescing leaves. *OsPAP26* mRNA in leaves, stems, roots and calli was maintained at a stable level irrespective of the status of Pi supply (**Fig. 1B**). To analyze *OsPAP26* expression more precisely in different tissues, transgenic rice plants that expressed a construct consisting of an *OsPAP26* promoter fused to a *β-glucuronidase* (*GUS*) reporter gene were generated. Five of these transgenic lines showed similar GUS expression patterns. As shown in **Fig. 1C**, strong GUS expression was detected in the leaves and roots of transgenic plants. Furthermore, GUS activities were not affected by Pi supply (data not shown).

To determine whether *OsPAP26* is regulated at the post-transcriptional level, a polyclonal antibody was raised and affinity purified against the *Escherichia coli* expressed OsPAP26 protein. Western blot analyses were carried out to determine the protein abundance in leaves and roots under Pi-replete and depleted conditions. As shown in **Fig. 1D**, OsPAP26 protein was markedly increased in leaves and roots under low Pi conditions. Our results indicated that the expression of OsPAP26 is regulated post-transcriptionally based on Pi supply.

Overexpression and RNA interference of *OsPAP26* altered APase activities in rice

To elucidate the function of OsPAP26, overexpression (Oe) and RNA interference (Ri) lines of *OsPAP26* were generated by *Agrobacterium*-mediated transformation. *OsPAP26* mRNA abundance was measured in a number of independent transgenic lines by qRT–PCR (**Fig. 2A**) and Western blot (**Fig. 2B**). As shown in **Fig. 2A** and **B**, the abundance of OsPAP26 transcript and protein was found to have increased in the Oe lines while it decreased in the Ri lines, as expected (**Fig. 2A, B**).

APase activities were measured in the leaf and root protein extracts of WT and transgenic lines. Under Pi-sufficient (+P) conditions, the leaf and root intracellular APases increased about 4-fold in *OsPAP26*-Oe rice compared with those in the WT (**Fig. 2C, D**). In contrast, the APase activities in *OsPAP26*-Ri plants significantly decreased in leaves and roots by 26–49%. In addition, Pi starvation (–P) significantly induced APase activities in WT, *OsPAP26*-overexpressing and RNAi plants.

Pi redistribution is altered in *OsPAP26*-overexpressing and RNAi plants

To assess the effect of OsPAP26 expression on Pi homeostasis, growth performance of *OsPAP26*-Oe and Ri plants was evaluated under +P and –P conditions. After 4 weeks of –P or +P treatments, the phenotypic differences among WT, Oe and Ri plants became visible. Under +P conditions, the growth performance and biomass of WT and Ri plants were similar, whereas Oe plants were slightly larger than WT and Ri plants. On the other hand, Ri plants showed significant growth inhibition compared with WT plants under –P conditions, and Oe plants were significantly larger than WT plants (**Fig. 3A**).

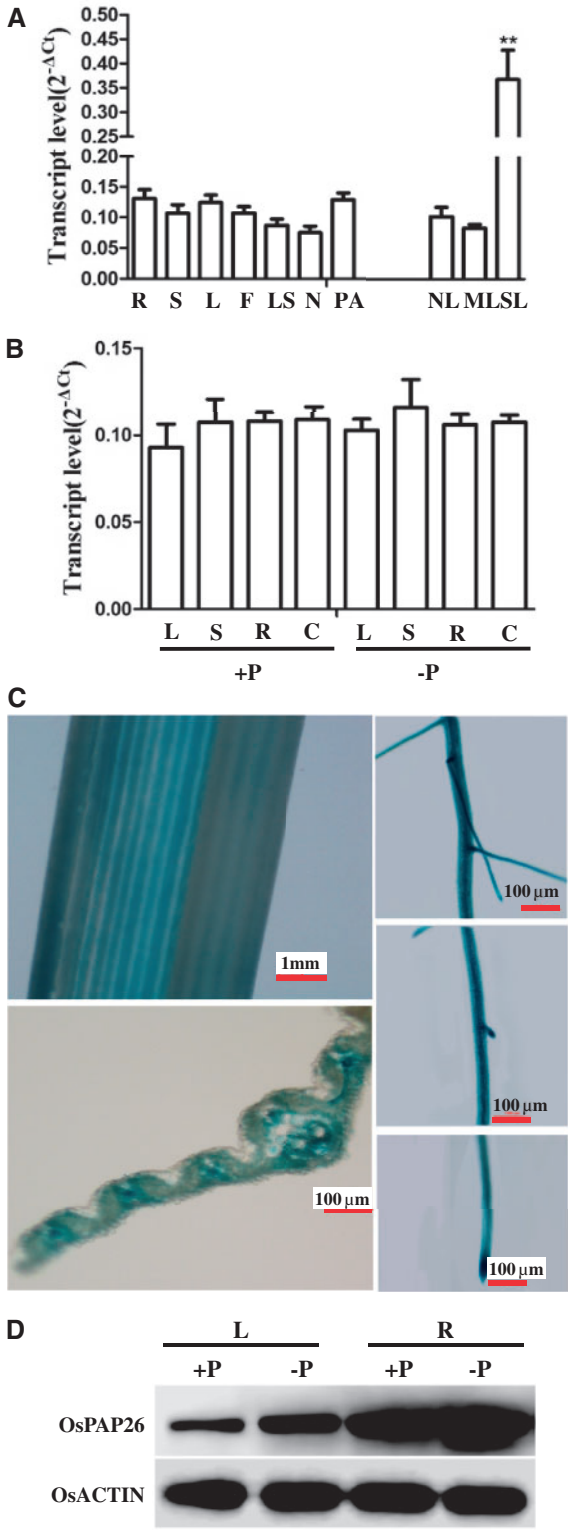

Fig. 1 Expression of *OsPAP26* in terms of transcription and protein levels. qRT–PCR results of *OsPAP26* in different tissues (A) and under various levels of Pi supply (B). The expression level of *OsPAP26* was normalized to *OsACTIN*. R, S, L, F, LS, N, PA, C, NL, ML and SL represent samples of roots, stems, leaves, flowers, leaf sheaths, nodes, panicles, calli, new leaves, mature leaves and senescing leaves, respectively. +P or −P represent samples grown under Pi-sufficient or deficient conditions, respectively. Values are presented as the mean ± SD (n = 3).

Leaf Pi concentrations in WT, *OsPAP26*-Oe and Ri plants were measured in new and senescing leaves of the plants grown in +P and −P conditions. To assess the changes of leaf Pi concentrations in the response to Pi deficiency, Pi concentrations of new and senescing leaves were measured at day 0 (before the treatment) and day 1, 2 and 3 after −P treatment. Results showed that overexpression of *OsPAP26* significantly increased Pi concentrations in new leaves compared with those in WT plants (**Fig. 3B**). In contrast, Pi concentrations in the senescing leaves were significantly lower in *OsPAP26*-Oe plants than in those of the WT plants in the +P condition (day 0) or after 1 d of Pi-deficient treatment (day 1, **Fig. 3B**). Prolonging Pi deficiency to 2–3 d minimized the difference. Repression of *OsPAP26* by RNAi resulted in marginal reduction of Pi concentrations in new leaves and an increase in senescing leaves compared with WT plants (**Fig. 3B**). Under the −P condition, there is no significant difference in the Pi concentrations of WT plants and *OsPAP26* RNAi lines in both new and senescing leaves (**Fig. 3B**) .

To analyze further the effect of OsPAP26 on Pi mobilization, Pi concentrations in a single leaf, labeled as the first to 10th, of WT, *OsPAP26*-Oe and Ri plants were measured. Pi concentrations gradually increased from the old to young leaves and then slightly decreased in the youngest leaves (the 10th leaf) (**Fig. 3C**). Compared with that in WT plants, the Pi concentration in the first leaf (senescing leaves) was lower in *OsPAP26*-Oe plants, but higher in Ri plants. In contrast, Pi concentrations in other leaves (the third to 10th leaves) were higher in the Oe plants and lower in the Ri plants compared with those of WT plants (**Fig. 3C**).

To verify the role of OsPAP26 in Pi mobilization, the abundance of OsPAP26 protein in leaves at different senescence stages was measured by Western blot. The results showed that senescing leaves accumulated more OsPAP26 protein than new or mature leaves in WT plants (**Fig. 4**). The higher accumulation of OsPAP26 in the senescing leaves implicated that OsPAP26 might play important roles in Pi remobilization in senescing leaves.

OsPAP26 is a major secreted APase in rice

AtPAP26 in Arabidopsis has been shown to be dual-targeted into the vacuole and secreted into the environment (Hurley et al. 2010). To determine the subcellular localization of OsPAP26, the *OsPAP26* gene was cloned downstream of the constitutive *Cauliflower mosaic virus* (CaMV) 35S promoter to create the *OsPAP26*–green fluorescent protein (GFP) fusion construct.

Fig. 1 Continued
Asterisks indicate significant differences from the mean value of non-senescing leaves by Student's *t*-test, $^{**}P < 0.01$. (C) GUS staining of the leaf (left) and roots (right) of 10-day-old POsPAP26-GUS transgenic seedlings. (D) Western blot of OsPAP26 in the leaves and roots of WT plants grown under +P or −P conditions. Two-week-old seedlings of WT rice were transferred to nutrient solution with or without Pi supply. Proteins were extracted from leaves or roots of rice plants after the 10 d treatment. ACTIN was used as loading control.

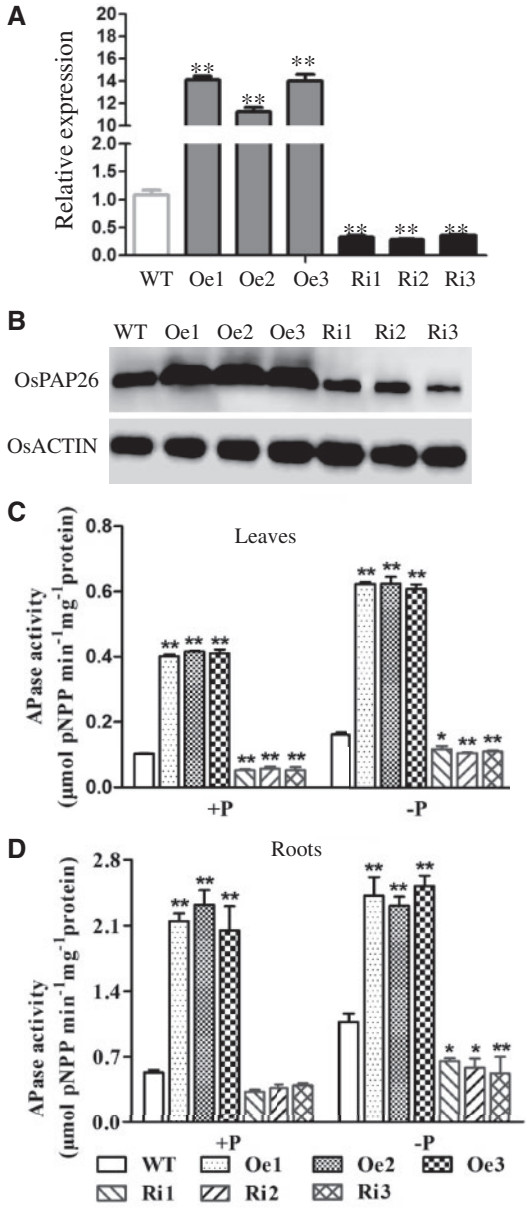

Fig. 2 Expression of OsPAP26 in wild-type and transgenic rice plants. qRT–PCR (A) and Western blot (B) of WT, *OsPAP26*-overexpressing (Oe) and RNA inteference (Ri) plants. (C and D) The APase activities in the leaves and roots of WT, Oe and Ri plants grown under +P and –P conditions, respectively. Two-week-old rice seedlings of WT, Oe and Ri were transferred to +P or –P conditions for 10 d prior to protein extraction. Hydrolysis of pNPP was used to measure APase activities. Values are presented as the mean ± SD (n = 3). Asterisks indicate significant differences from the mean value of the WT by Student's t-test, $^{*}P < 0.05$ or $^{**}P < 0.01$.

GFP signals were observed in the apoplast expressing the construct (**Fig. 5A**), suggesting that OsPAP26 is probably a secreted protein. To confirm further that OsPAP26 can be secreted into the extracellular environment, suspension cultures derived from the WT and the *OsPAP26*-Oe and Ri transgenic calli were established. Proteins in the culture media were then harvested and concentrated. Western blot detected substantial amount of OsPAP26 in the medium protein extracts, which confirmed that OsPAP26 is indeed a secreted APase (**Fig. 5B**). In addition, Pi starvation induced OsPAP26 SAP proteins and APase activities, which were observed not only in the WT, but also in the *OsPAP26*-overexpressing and RNAi lines (**Figs. 4C, 5B**).

To investigate the function of the secreted OsPAP26 protein, ATP degradation ability was measured in *OsPAP26*-overexpressing lines. In WT plants, ATP was gradually degraded from day 1 to day 6 and nearly 20% free Pi was released at day 4 (**Fig. 5D**). Compared with the WT, overexpression of OsPAP26 significantly increased Pi release from ATP at day 2 and released >50% free Pi after day 3 (**Fig. 5D**). Thus, we concluded that overexpression of OsPAP26 could increase Pi release from ATP.

Discussion

PAPs hydrolyze extracellular organic P sources into an inorganic form, and were therefore considered to be important for plant adaptation to low Pi conditions. In this study, we demonstrated that OsPAP26 is a secreted PAP and can trigger extracellular ATP degradation. The extracellular APase activity of OsPAP26 is important for the utilization of rhizosphere organic P or for the recycling of organic P from cell walls in response to Pi deficiency stress. Our observation that OsPAP26 protein was up-regulated by Pi starvation supports the role of OsPAP26 in the hydrolysis of organic P (**Fig. 1D**). In addition, our study also showed that OsPAP26 is expressed at a higher level in senescing leaves than in non-senescing leaves (**Fig. 1D**). Alteration of OsPAP26 expression by genetic engineering affected the Pi distribution in both senescing and non-senescing leaves (**Fig. 3B, C**). These results support that OsPAP26 plays an important role in Pi remobilization from senescing leaves to young leaves.

Many studies of plant PAPs focused on the PAPs whose expression was transcriptionally induced by a Pi depletion or Pi starvation signal as controlled by the central transcription factor PHR (AtPHR1 or OsPHR2). Indeed, many of these transcriptionally regulated *PAP* genes play important roles in plant adaptation to Pi depletion stress (Miller et al. 2001, Bozzo et al. 2002, Bozzo et al. 2004a, Bozzo et al. 2004b, Bozzo et al. 2006, Wang et al. 2011, Tian et al. 2012, Lu et al. 2016). Expression of 11, 10, 10 and 22 *PAP* genes is transcriptionally induced by Pi starvation in Arabidopsis, rice, maize and soybean, respectively (Zhang et al. 2011, Li et al. 2012, Gonzalez-Munoz et al. 2015). However, these Pi starvation-induced PAPs only account for >40% of all PAP members. In addition, some PAP members are induced post-transcriptionally. For instance, upon Pi starvation, AtPAP26 protein accumulation increased, with no change in its transcript abundance (Veljanovski et al. 2006). In this study, we found that the expression of the AtPAP26 ortholog, OsPAP26, is also up-regulated post-transcriptionally in response to Pi starvation (**Fig. 1D**). Tran et al. (2010) have discussed some possible mechanisms of post-transcriptional regulation of plant PAPs, including splice variants (e.g. AtPAP10; Li et al. 2002), reversible protein phosphorylation

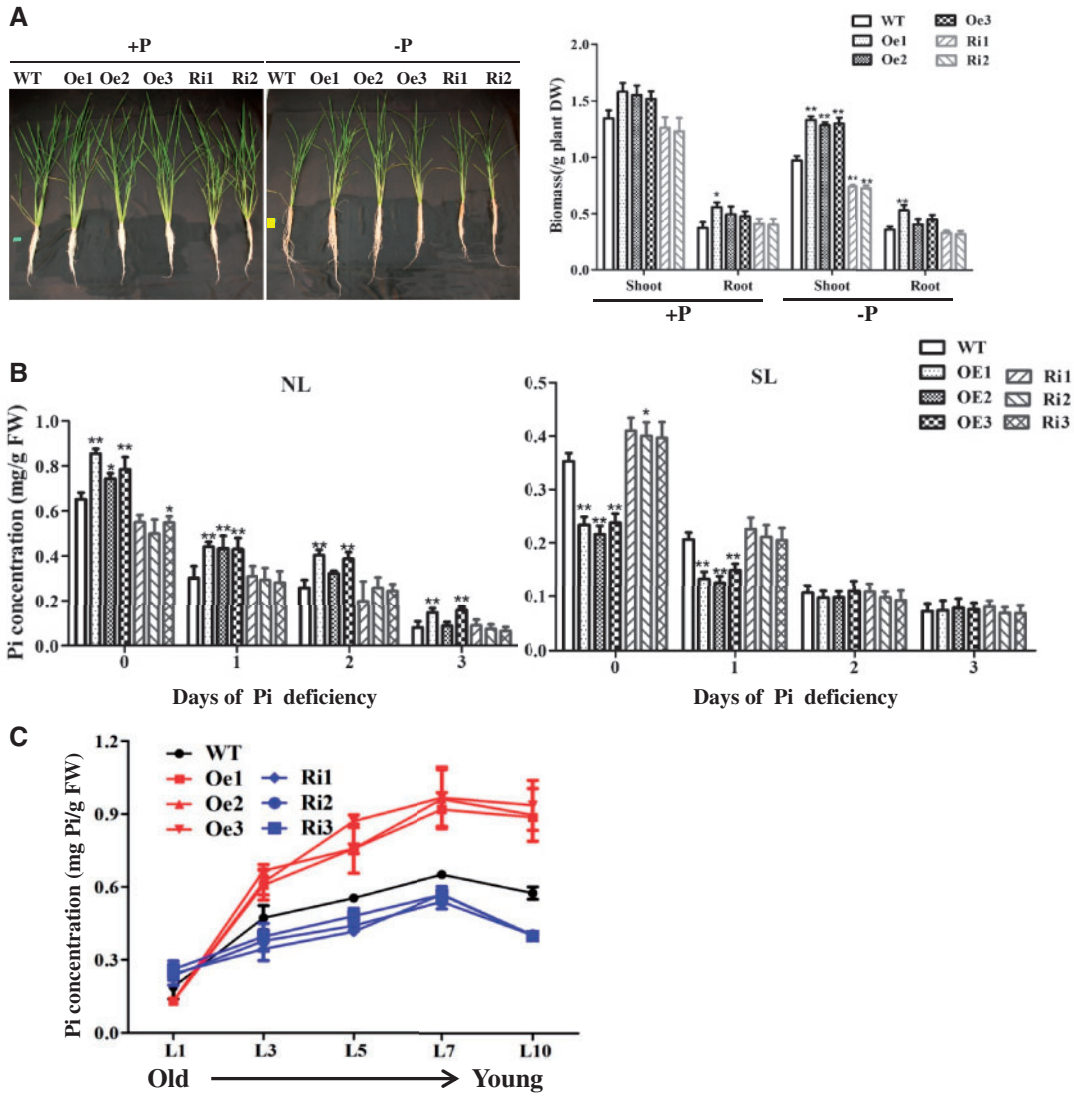

Fig. 3 Growth performance and Pi accumulation of WT, *OsPAP26*-Oe and Ri plants. (A) Growth performance and biomass of WT, Oe and Ri plants grown under +P and −P conditions. Scale bar = 3.5 cm. Two-week-old seedlings were transferred to nutrient solution with or without supplies of Pi for 4 weeks. (B) Pi concentrations of WT, Oe and Ri plants grown under +P and −P conditions. Two-week-old seedlings were transferred to nutrient solution until the 10-leaf stage. Pi concentrations of the new (NL) and senescing leaves (SL) were measured at day 0, 1, 2 and 3 of the −P treatment. (C) Pi concentrations in different leaves of the 8-week-old WT, Oe and Ri plants. Oe1, Oe2, Oe3, *OsPAP10c*-overexpressing lines 1–3; Ri1, Ri2, Ri3, *OsPAP10c* RNAi lines 1–3. Values are presented as the mean ± SD (n = 3). Asterisks indicate significant differences from the mean value of the WT by Student's t-test, $^{*}P < 0.05$ or $^{**}P < 0.01$.

and serine proteases for degradation of PSI tomato PAPs upon supplying Pi to −Pi cells (Bozzo et al. 2004b). Recent studies showed that post-translational control of Pi transporters at the level of protein stability also plays very important roles in Pi uptake and homeostasis. This process involves the ubiquitin-mediated protein degradation pathway (Huang et al. 2013, Lin et al. 2013, Park et al. 2014, Ying et al. 2016) and kinase(s)-mediated protein phosphorylation (Chen et al. 2015). However, future studies are needed to clarify the detailed mechanism of the post-transcriptional regulation of OsPAP26.

Recent studies have demonstrated the important function of *AtPAP26* in the adaptation to Pi stress through encoding the major IAP and SAP in Arabidopsis (Hurley et al. 2010). Although orthologs of *AtPAP26* exist in various plants, the functions of these orthologous genes are largely unknown. In this study, overexpression of *OsPAP26* not only increased the APase activities in various plant tissues, but also elevated Pi concentrations in the functional leaves (young leaves and mature leaves; **Fig. 3B, C**). We found that the high accumulation of OsPAP26 protein in senescing leaves triggers Pi remobilization from the senescing leaves to young leaves (**Fig. 3D**). Consequently, these *OsPAP26*-Oe plants adapted to Pi deficiency significantly better than the WT in a hydroponic study (**Fig. 3A**). In contrast, growth of the *OsPAP26*-Ri plants was significantly weaker than that of WT plants. It is likely that the disruption of Pi remobilization in the Ri plants further aggravated the Pi deficiency stress. A well-controlled field trial focusing on evaluation of agronomic performance of these

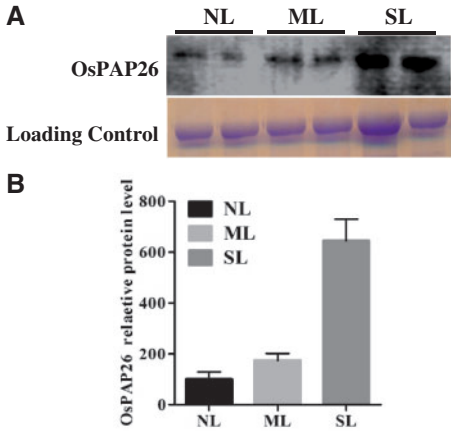

Fig. 4 Western blot of OsPAP26 in new, mature and senescing leaves of WT plants. Leaf protein extracts were loaded in duplicate for Western blot analysis.

OsPAP26-Oe plants should be conducted to assess the breeding value of a corresponding transgene for generation of crops that more efficiently utilize P.

Materials and Methods

Plant material and growth conditions

Cultivar 'Nipponbare' of *Oryza sativa* was used for all physiological experiments and rice transformations. Hydroponic experiments were conducted using a modified rice culture solution as previously described (Wang et al. 2012). The Pi-sufficient culture solution contained 1.425 mM NH_4NO_3, 0.323 mM NaH_2PO_4, 0.513 mM K_2SO_4, 0.998 mM $CaCl_2$, 1.643 mM $MgSO_4$, 0.25 mM $NaSiO_3$, 0.009 mM $MnCl_2$, 0.075 µM $(NH_4)_6Mo_7O_{24}$, 0.019 µM H_3BO_3, 0.155 µM $CuSO_4$ and 0.152 µM $ZnSO_4$ with 0.125 mM EDTA-Fe (II). For −P treatment, Pi was eliminated from the nutrient solution. The pH of all nutrient solutions was adjusted to 5.5. Rice seedlings were grown in growth chambers with a 12 h photoperiod (200 µmol photons m^{-2} s^{-1}) and a day/night temperature of 30/22°C after germination. Humidity was maintained at 60% relative humidity.

For ATP degradation experiments, 0.5 mM ATP was added to the nutrient solution to replace the 0.323 mM NaH_2PO_4.

RNA preparation and qRT–PCR

Total RNA was extracted from the leaves and roots using Trizol reagent following the manufacturer's instructions (Invitrogen). RNA samples were collected in three biological replicates. First-strand cDNAs were synthesized from total RNA using M-MLV reverse transcriptase (Promega). qRT–PCR was performed using a LightCycler 480 SYBR Green I Master Kit on a LightCycler480 machine (Roche Diagnostics) according to the manufacturer's instructions. Transcript levels were calculated relative to *OsACTIN1* using the formula $2^{-}\Delta^{Ct}$. The primers are listed in Supplementary Table S1.

Construction of vectors and plant transformation

The *OsPAP26* overexpression, RNAi and the *OsPAP26* promoter-fused *GUS* reporter gene (POsPAP26-GUS) vectors were constructed and introduced to the Nipponbare rice background as previously described (Wang et al. 2012). In brief, full-length *OsPAP26* was cloned and inserted into the pTF101-ubi vector for overexpression (Zheng et al. 2010). To generate *OsPAP26* RNAi lines, a 250 bp fragment encompassing nucleotides 335–585 of the *OsPAP26* coding sequence was amplified and sequentially cloned in the opposite orientation to generate a double-stranded RNA with a hairpin structure via homologous recombination into the gateway vector pB7GWIW2. For the POsPAP26-GUS lines, the promoter region of a 2.5 kb fragment upstream of the start codon ATG was amplified from the Nipponbare genomic DNA fragments. The purified PCR product was cloned into the binary vector pBIGUS-plus using a GBclonart Seamless Assembly Kit according to the manufacturer's instructions (GBI). Transgenic lines were produced with resulted plasmids POsPAP26-GUS via *Agrobacterium*-mediated rice transformation. The primers are listed in Supplementary Table S1.

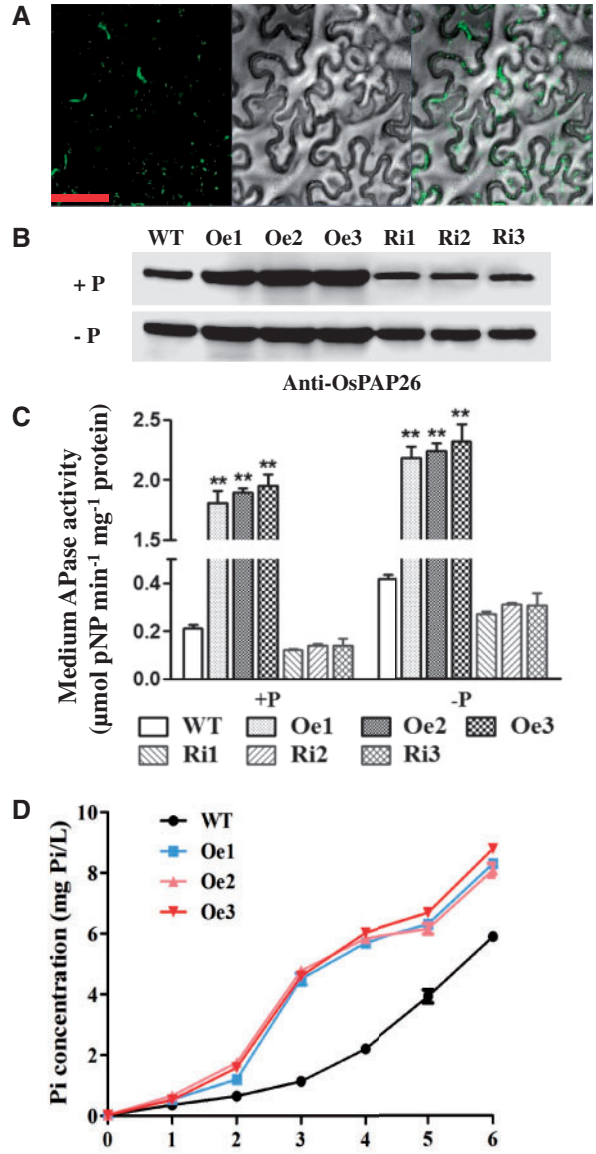

Fig. 5 Confirmation of OsPAP26 as a secreted protein. (A) Subcellular localization of OsPAP26–GFP in tobacco epidermal cells. Scale bar = 100 µm. Western blot (B) and APase activities (C) of protein extracts from growth media of WT, *OsPAP26*-Oe and *OsPAP26*-Ri calli. Calli of WT and transgenic lines were generated and suspended in +P or −P medium for a week. Proteins were extracted and concentrated from the culture media. Values are presented as the mean ± SD (n = 3). Asterisks indicate significant differences from the mean value of the WT by Student's t-test, $^*P < 0.05$ or $^*P < 0.01$. (D) Pi concentrations of nutrient solution in which the WT, *OsPAP26*-Oe and *OsPAP26*-Ri plants were grown. The hydroponic medium contained 0.1 mM ATP as the only source of phosphorus. Pi concentrations of the solution were measured daily during treatment. Values are presented as the mean ± SD (n = 5).

Protein extraction from plant tissues and culture media

Root and leaf tissues were ground separately into fine powders in liquid nitrogen and then homogenized in ice-cold extraction buffer containing 0.1 M potassium acetate, 20 mM $CaCl_2$, 2 mM EDTA and 0.1 mM phenylmethylsulfonyl fluoride at pH 5.5. Samples were gently agitated on ice for 30 min and then centrifuged at 14,000×*g* at 4 °C for 20 min. The supernatant was transferred to a fresh tube before use. The protein content was quantified using Coomassie Plus protein assay reagent.

Preparation of culture media from suspended rice calli was performed as described previously (Lu et al. 2016). Proteins were concentrated and isolated using centrifugal filter devices with a 3 kDa cut-off at 4 °C according to the manufacturer's instructions (Merck KgaA). Protein content was quantified using Coomassie Plus protein assay reagent.

Western blot analysis of OsPAP26 proteins

To raise antibodies against OsPAP26, the open reading frame of *OsPAP26* was amplified and inserted into the expression vector pET-30a. OsPAP26 protein was purified from *E. coli* cells containing the above vector. An anti-OsPAP26 polyclonal rabbit antibody was raised and affinity purified against the immunogenic sequence. The final concentration of affinity-purified antibodies used for the immunoblot analyses was 1 : 500 (v/v). An antibody against ACTIN was purchased from Earthox LLC, USA (Plant-ACTIN Rabbit Polyclonal Antibody).

For Western blot, protein samples were separated on 10% SDS–polyacrylamide gels, and transferred to a polyvinylidene fluoride (PVDF) membrane in transfer buffer (123.8 mM Tris, 77.26 mM glycine, 1.28 mM SDS and 20% methanol). The membrane was blocked with 5% milk in TBST (Tris-buffered saline with Tween-20) buffer at room temperature for 1 h and then incubated with OsPAP26 antibodies (1 : 500) at room temperature for 1 h in TBST buffer containing 0.5% milk. Next, the membrane was incubated with horseradish peroxidase-conjugated goat anti-rabbit antibody at 1 : 10,000 dilution for 1 h. During the incubation, the membrane was washed with TBST six times, each for 5 min. After all antibody incubation steps were completed, the membrane was washed three times with TBST (5 min each) and incubated for 5 min at room temperature in a mixture (1 : 1) of the two enhanced chemiluminescence solutions. The blotted membrane was analyzed using a C-digit Chemiluminescent WesternBlot Scanner (LI-COR).

Measurement of APase activities

To measure specific APase activity, 1 μg (root and medium protein extracts) or 10 μg (leaf protein extracts) of proteins were added to 600 μl of pre-warmed 10 mM pNPP (*p*-nitrophenyl phosphate) in 50 mM sodium acetate at pH 5.5. Reactions were allowed to proceed for 30 min (root and leaf) or 10 min (medium) at 25 °C and then stopped with 1.2 ml of 1 M NaOH. Absorbance at 410 nm was determined using a Spectroquant NOVA60 spectrophotometer (Merck).

β-Glucuronidase (GUS) histochemical analysis

The T_1 seeds of POsPAP26-GUS transgenic plants were grown in nutrient solutions. Different tissues were sampled for GUS staining as described previously. In brief, plant tissues from GUS transgenic lines were immediately submerged in GUS staining solution upon harvest and kept under a vacuum for 10 min. The stained sections were incubated at 37 °C for 2 h, washed in 70% ethanol for Chl removal and observed under a stereoscope. For sections, the roots and leaves were embedded in 3% agar and cut into 30 μm sections using a vibrating microtome (Leica VT1000S). They were then examined and photographed through a microscope (Nikon).

Subcellular localization of OsPAP26

The full-length cDNA of *OsPAP26* was fused to the 5′ end of GFP in-frame. The OsPAP26::GFP fragment was then cloned downstream of the constitutive CaMV 35S promoter to create the 35S-OsPAP26::GFP fusion construct. The resulting construct was transiently expressed in tobacco leaves by *Agrobacterium*-mediated infiltration as described previously (Walter et al. 2004). GFP fluorescence of tobacco leaves was assessed 2 d after infiltration using a LSM710 NLO confocal laser scanning microscope (Carl Zeiss).

Measurement of Pi concentration

Leaves and roots of the WT and transgenic seedlings from different treatments were sampled separately. Pi concentration was measured using the procedure described previously. Briefly, 50 mg of fresh tissue was homogenized in 50 μl of 5 M H_2SO_4 and 3 ml of H_2O. The homogenate was transferred to 1.5 ml tubes and centrifuged at 10,000×*g* for 10 min at 4 °C. The supernatant was collected and diluted to an appropriate concentration. The diluted supernatant was mixed with a malachite green reagent in a 3 : 1 ratio and analyzed 20 min afterwards. The absorption values for the solution at 650 nm were determined using a Spectroquant NOVA60 spectrophotometer (Merck). Pi concentration was calculated from a standard curve generated with various concentrations of KH_2PO_4.

Statistical analysis

Data were statistically analyzed using the Data Processing System (DPS Version 7.05). Student's *t*-test was performed to determine the significance of differences between the WT and the transgenic lines in each treatment.

Supplementary data

Supplementary data are available at PCP online.

Funding

This work was supported by the Ministry of Science and Technology of China [2016YFD0100703, 2016ZX08003005-001 and 2014ZX08009328-002]; the National Natural Science Foundation of China [31572189, 31401934 and 31471929]; the Ministry of Education of China [111 project; B14027]; and the Natural Science Foundation of Zhejiang Province [LZ16C150001].

Disclosures

The authors have no conflicts of interest to declare.

References

Boutin, J.P., Provot, M. and Roux, L. (1981) Effect of cycloheximide and renewal of phosphorus supply on surface acid phosphatase activity of phosphorus deficient tomato roots. *Physiol. Plant.* 51: 353–360.

Bozzo, G.G., Dunn, E.L. and Plaxton, W.C. (2006) Differential synthesis of phosphate-starvation inducible purple acid phosphatase isozymes in tomato (Lycopersicon esculentum) suspension cells and seedlings. *Plant Cell Environ.* 29: 303–313.

Bozzo, G.G., Raghothama, K.G. and Plaxton, W.C. (2002) Purification and characterization of two secreted purple acid phosphatase isozymes from phosphate-starved tomato (Lycopersicon esculentum) cell cultures. *Eur. J. Clin. Chem.* 269: 6278–6286.

Bozzo, G.G., Raghothama, K.G. and Plaxton, W.C. (2004a) Structural and kinetic properties of a novel purple acid phosphatase from phosphate-starved tomato (Lycopersicon esculentum) cell cultures. *Biochem. J.* 377: 419–428.

Bozzo, G.G., Singh, V.K. and Plaxton, W.C. (2004b) Phosphate or phosphite addition promotes the proteolytic turnover of phosphate-starvation inducible tomato purple acid phosphatase isozymes. *FEBS Lett.* 573: 51–54.

Chen, J.Y., Wang, Y., Wang, F., Yang, J., Gao, M., Li, C., et al. (2015) The rice CK2 kinase regulates trafficking of phosphate transporters in response to phosphate levels. *Plant Cell.* 27: 711–723.

del Pozo, J.C., Allona, I., Rubio, V., Leyva, A., De La Peña, A., Aragoncillo, C., et al. (1999) A type 5 acid phosphatase gene from Arabidopsis thaliana is induced by phosphate starvation and by some other types of phosphate mobilising/oxidative stress conditions. *Plant J.* 19: 579–589.

Del Vecchio, H.A., Ying, S., Park, J., Knowles, V.L., Kanno, S., Tanoi, K., et al. (2014) The cell wall-targeted purple acid phosphatase AtPAP25 is critical for acclimation of Arabidopsis thaliana to nutritional phosphorus deprivation. *Plant J.* 80: 569–581.

Dionisio, G., Madsen, C.K., Holm, P.B., Welinder, K.G., Jørgensen, M., Stoger, E., et al. (2011) Cloning and characterization of purple acid phosphatase phytases from wheat, barley, maize, and rice. *Plant Physiol.* 156: 1087–1100.

González-Muñoz, E., Avendaño-Vázquez, A.O., Montes, R.A.C., de Folter, S., Andrés-Hernández, L., Abreu-Goodger, C., et al. (2015) The maize (Zea mays ssp. mays var. B73) genome encodes 33 members of the purple acid phosphatase family. *Front. Plant Sci.* 6. 341.

Haran, S., Logendra, S., Seskar, M., Bratanova, M. and Raskin, I. (2000) Characterization of Arabidopsis acid phosphatase promoter and regulation of acid phosphatase expression. *Plant Physiol.* 124: 615–626.

Huang T.K., Han, C.L., Lin, S.I., Chen, Y.J., Tsai, Y.C., Chen, Y.R., et al. (2013). Identification of downstream components of ubiquitin-conjugating enzyme PHOSPHATE2 by quantitative membrane proteomics in Arabidopsis roots. *Plant Cell* 25: 4044–4060.

Hurley, B.A., Tran, H.T., Marty, N.J., Park, J., Snedden, W.A., Mullen, R.T., et al. (2010) The dual-targeted purple acid phosphatase isozyme AtPAP26 is essential for efficient acclimation of Arabidopsis to nutritional phosphate deprivation. *Plant Physiol.* 153: 1112–1122.

Kuang, R., Chan, K.H., Yeung, E. and Lim, B.L. (2009) Molecular and biochemical characterization of AtPAP15, a purple acid phosphatase with phytase activity, in Arabidopsis. *Plant Physiol.*151: 199–209.

Li, C., Gui, S., Yang, T., Walk, T., Wang, X. and Liao, H. (2012) Identification of soybean purple acid phosphatase genes and their expression responses to phosphorus availability and symbiosis. *Ann. Bot.* 109: 275–285.

Li, D., Zhu, H., Liu, K., Liu, X., Leggewie, G., Udvardi, M., et al. (2002) Purple acid phosphatases of Arabidopsis thaliana. Comparative analysis and differential regulation by phosphate deprivation. *J. Biol. Chem.* 277: 27772–27781.

Liang, C., Tian, J., Lam, H.M., Lim, B.L., Yan, X. and Liao, H. (2010) Biochemical and molecular characterization of PvPAP3, a novel purple acid phosphatase isolated from common bean enhancing extracellular ATP utilization. *Plant Physiol.* 152: 854–865.

Lin, W.Y., Huang, T.K. and Chiou, T.J. (2013). Nitrogen limitation adaptation, a target of microRNA827, mediates degradation of plasma membrane-localized phosphate transporters to maintain phosphate homeostasis in Arabidopsis. *Plant Cell* 25: 4061–4074.

Lu, L., Qiu, W., Gao, W., Tyerman, S.D., Shou, H. and Wang, C. (2016) OsPAP10c, a novel secreted acid phosphatase in rice, plays an important role in the utilization of external organic phosphorus. *Plant Cell Environ.* 39: 2247–2259.

McLachlan, K.D. (1980) Acid phosphatase activity of intact roots and phosphorus nutrition in plants. 1. Assay conditions and phosphatase activity. *Crop Pasture Sci.* 31: 429–440.

Miller, S.S., Liu, J., Allan, D.L., Menzhuber, C.J., Fedorova, M. and Vance, C.P. (2001) Molecular control of acid phosphatase secretion into the rhizosphere of proteoid roots from phosphorus-stressed white lupin. *Plant Physiol.* 127: 594–606.

Olczak, M., Morawiecka, B. and Watorek, W. (2003) Plant purple acid phosphatases—genes, structures and biological function. *Acta Biochim. Pol.* 50: 1245–1256.

Park, B.S., Seo, J.S. and Chua, N.H. (2014). NITROGEN LIMITATION ADAPTATION recruits PHOSPHATE2 to target the phosphate transporter PT2 for degradation during the regulation of Arabidopsis phosphate homeostasis. *Plant Cell* 26: 454–464.

Schenk, G., Guddat, L.W., Ge, Y., Carrington, L.E., Hume, D.A., Hamilton, S., et al. (2000) Identification of mammalian-like purple acid phosphatases in a wide range of plants. *Gene* 250: 117–125.

Silberbush, M., Shomer-Ilan, A. and Waisel, Y. (1981) Root surface phosphatase activity in ecotypes of Aegilops peregrina. *Physiol. Plant.* 53: 501–504.

Tang, H., Li, X., Zu, C., Zhang, F. and Shen, J. (2013) Spatial distribution and expression of intracellular and extracellular acid phosphatases of cluster roots at different developmental stages in white lupin. *J. Plant Physiol.* 170: 1243–1250.

Tian, J., Wang, C., Zhang, Q., He, X., Whelan, J. and Shou, H. (2012) Overexpression of OsPAP10a, a root-associated acid phosphatase, increased extracellular organic phosphorus utilization in rice. *J. Integr. Plant Biol.* 54: 631–639.

Tran, H.T., Qian, W., Hurley, B.A., She, Y.M., Wang, D. and Plaxton, W.C. (2010) Biochemical and molecular characterization of AtPAP12 and AtPAP26: the predominant purple acid phosphatase isozymes secreted by phosphate-starved Arabidopsis thaliana. *Plant Cell Environ.* 33: 1789–1803.

Veljanovski, V., Vanderbeld, B., Knowles, V.L., Snedden, W.A. and Plaxton, W.C. (2006) Biochemical and molecular characterization of AtPAP26, a vacuolar purple acid phosphatase up-regulated in phosphate-deprived Arabidopsis suspension cells and seedlings. *Plant Physiol.* 142: 1282–1293.

Walter, M., Chaban, C., Schütze, K., Batistic, O., Weckermann, K., Näke, C., et al. (2004) Visualization of protein interactions in living plant cells using bimolecular fluorescence complementation. *Plant J.* 40: 428–438.

Wang, X., Wang, Y., Tian, J., Lim, B.L., Yan, X. and Liao, H. (2009) Overexpressing AtPAP15 enhances phosphorus efficiency in soybean. *Plant Physiol.* 151: 233–240.

Wang, C., Huang, W., Ying, Y., Li, S., Secco, D., Tyerman, S., et al. (2012) Functional characterization of the rice SPX-MFS family reveals a key role of OsSPX-MFS1 in controlling phosphate homeostasis in leaves.*New Phytol.* 196: 139–148.

Wang, L., Li, Z., Qian, W., Guo, W., Gao, X., Huang, L., et al. (2011) The Arabidopsis purple acid phosphatase AtPAP10 is predominantly associated with the root surface and plays an important role in plant tolerance to phosphate limitation. *Plant Physiol.* 157: 1283–1299.

Wang, L., Lu, S., Zhang, Y., Li, Z., Du, X. and Liu, D. (2014) Comparative genetic analysis of Arabidopsis purple acid phosphatases AtPAP10, AtPAP12, and AtPAP26 provides new insights into their roles in plant adaptation to phosphate deprivation. *J. Integr. Plant Biol.* 56: 299–314.

Ying, Y.H., Yue, W., Wang, S., Li, S., Wang, M., Zhao, Y., et al. (2016) Two h-type thioredoxins interact with the PHO2 ubiquitin-conjugating E2 enzyme to fine-tune phosphate homeostasis. *Plant Physiol.* 173: 812–824

Zhang, Q., Wang, C., Tian, J., Li, K. and Shou, H. (2011) Identification of rice purple acid phosphatases related to phosphate starvation signalling. *Plant Biol.* 13: 7–15.

Zhang, W., Gruszewski, H.A., Chevone, B.I. and Nessler, C.L. (2008) An Arabidopsis purple acid phosphatase with phytase activity increases foliar ascorbate. *Plant Physiol.* 146: 431–440.

Zhang, Y., Wang, X., Lu, S. and Liu, D. (2014) A major root-associated acid phosphatase in Arabidopsis, AtPAP10, is regulated by both local and systemic signals under phosphate starvation. *J. Exp. Bot.* 65: 6577–6588.

Zheng, L., Cheng, Z., Ai, C., Jiang, X., Bei, X., Zheng, Y., et al. (2010) Nicotianamine, a novel enhancer of rice iron bioavailability to humans. *PLoS One.* 5: e10190.

Zhu, H., Qian, W., Lu, X., Li, D., Liu, X., Liu, K., et al. (2005) Expression patterns of purple acid phosphatase genes in Arabidopsis organs and functional analysis of AtPAP23 predominantly transcribed in flower. *Plant Mol. Biol.* 59: 581–594.